Thin Solid Films 518 (2010) 6149–6152

Contents lists available at ScienceDirect

Thin Solid Films

journal homepage: www.elsevier.com/locate/tsf

Electron injection mechanisms of green organic light-emitting devices fabricated utilizing a double electron injection layer consisting of cesium carbonate and fullerene

J.S. Yang [a], D.C. Choo [b], T.W. Kim [a,b,*], Y.Y. Jin [c], J.H. Seo [c], Y.K. Kim [c]

[a] Department of Information Display Engineering, Hanyang University, Seoul 133-791, South Korea
[b] Department of Electronics and Computer Engineering, Hanyang University, Seoul 133-791, South Korea
[c] Department of Information Display Engineering & Center for Organic Materials & Information Display (COMID), Hong-ik University, Seoul 121-791, South Korea

ARTICLE INFO

Available online 29 April 2010

Keywords:
Organic light-emitting devices
Cesium carbonate
Fullerene
Double electron injection layer

ABSTRACT

Electron injection mechanisms of the luminance efficiency of green organic light-emitting devices (OLEDs) fabricated utilizing a cesium carbonate (Cs_2CO_3)/fullerene (C_{60}) heterostructure acting as an electron injection layer (EIL) were investigated. Current density–voltage and luminance–voltage measurements showed that the current densities and the luminances of the OLEDs with a Cs_2CO_3 or Cs_2CO_3/C_{60} EIL were higher than that of the OLEDs with a Liq EIL. The luminance efficiency of the OLEDs with a Cs_2CO_3 EIL was almost three times higher than that of the OLEDs with a Liq EIL. Because the electron injection efficiency of the Cs_2CO_3 layer in OLEDs was different from that of the C_{60} layer, the luminance efficiency of the OLEDs with a double EIL consisting of a Cs_2CO_3 layer and a C_{60} layer was smaller than that of the OLEDs with a Cs_2CO_3 EIL. The electron injection mechanisms of OLEDs with a Cs_2CO_3 and C_{60} double EIL are described on the basis of the experimental results.

1. Introduction

Organic light-emitting devices (OLEDs) have emerged as excellent candidates for potential applications in promising next-generation full-color flat-panel displays because they have superior device advantages of low driving voltage, high contrast, fast response, and wide viewing angle [1–5]. Moderate controls of carrier injection and transport for efficient carrier recombination and balance of the electrons and the holes in the emitting layer (EML) are necessary to fabricate high-efficiency OLEDs [6–8]. Because the hole mobility is organic layers typically higher than their electron mobility, an increase in the electron injection is necessary to enhance the luminance efficiency of the OLEDs. Some works concerning the fabrications, the physical properties, and the luminance mechanisms of OLEDs with a lithium fluoride (LiF)/Al, a lithium quinolate (Liq)/Al, or a cesium fluoride (CsF)/Al cathode have been performed to enhance the efficiency of the OLEDs [9–11]. Some works on the enhancement of the efficiency in green OLEDs with various electron injection layers (EILs) have been performed [12–15]. However, systematic studies concerning the enhancement mechanisms of the luminance efficiency in OLEDs fabricated utilizing a heterostructure EIL are very important for improving the efficiencies of the OLEDs. Even though some studies on the enhancement of electron injection due to the insertion of Cs_2CO_3 EIL have been preformed [16], works concerning the improvement of the electron injection and Cs diffusion from Cs_2CO_3 have not been clearly clarified yet.

This paper reports enhancement mechanisms of the luminance efficiency in green OLEDs fabricated utilizing a Cs_2CO_3/C_{60} heterostructure acting as an EIL fabricated by using organic thermal deposition. Current density–voltage, luminance–voltage, and luminance efficiency–current density measurements were carried out to investigate the electrical and the optical properties of the OLEDs with various EILs. The optical and electrical properties of green OLEDs with a Cs_2CO_3/C_{60} EIL heterostructure were compared with those of OLEDs with a single Liq or Cs_2CO_3 EIL.

2. Experimental details

The sheet resistivity and the thickness of the indium–tin-oxide (ITO) thin films coated on glass substrates used in this study were 15 Ω/square and 100 nm, respectively. The ITO substrates were cleaned using sonication in acetone, methanol, and distilled water at 27 °C for 15 min. The chemically cleaned ITO substrates were kept for 48 h in isopropyl alcohol. After the chemically cleaned ITO substrates had been dried by using N_2 gas with a purity of 99.9999%, the surfaces of the ITO substrates were treated with an oxygen plasma for 2 min at an O_2 pressure of approximately 2×10^{-2} Torr. The three kinds of devices were deposited on ITO-coated glass substrates at a chamber

* Corresponding author. Department of Electronics and Computer Engineering, Hanyang University, Seoul 133-791, South Korea.
E-mail address: twk@hanyang.ac.kr (T.W. Kim).

0040-6090/$ – see front matter © 2010 Elsevier B.V. All rights reserved.
doi:10.1016/j.tsf.2010.04.061

pressure of 3×10^{-6} Torr and consisted of the following structures from the top: an Al (100 nm) cathode electrode, various kinds of the EILs, a 4,7-diphenyl-1,10-phenanthroline (BPhen) (30 nm) electron transport layer (ETL), an 8 wt% fac-tris(2-phenylpyridine) iridium ($Ir(ppy)_3$) doped 4,4′-bis(N-carbazolyl)biphenyl (CBP) (30 nm) emissive layer (EML), an N,N′-Bis(naphthalene-1-yl)-N,N′-bis(phenyl)-benzidine (NPB) (50 nm) hole transport layer (HTL), an ITO anode electrode, and a glass substrate. Three kinds of EILs for OLEDs consisted of a Liq (2 nm), a Cs_2CO_3 (2 nm), or Cs_2CO_3 (2 nm)/C_{60} (2 nm). Three kinds of electron only devices (EODs) also were deposited on ITO-coated glass substrates at a chamber pressure of 3×10^{-6} Torr and consisted of the following structures from the top: Al (100 nm) cathode electrode, various kinds of the EILs, a 4,7-diphenyl-1,10-phenanthroline (BPhen) (30 nm) ETL, a 2,9-dimethyl-4,7-diphenyl-phenanthroline (BCP) hole blocking layer (HBL) (30 nm), an ITO anode electrode, and a glass substrate. Three kinds of EILs for EODs consisted of a Liq (2 nm), a Cs_2CO_3 (2 nm), or Cs_2CO_3 (2 nm)/C_{60} (2 nm). The fabrications of the OLEDs and the EODs were completed with encapsulation in a glove box under O_2 and H_2O concentrations below 1 ppm. The residual moisture and oxygen in the encapsulated device were absorbed by a desiccant consisting of barium-oxide powder. The evaporation rates of the organic layers and the Al cathode were approximately 0.1 and 0.15 nm/s, respectively. The deposition rates were controlled by using a quartz crystal monitor. The emitting area in the pixel was 3×3 mm^2. The current density–voltage characteristics of the OLEDs were measured on a programmable electrometer with built-in current and voltage measurement units (SMU-236, Keithely). The luminance was measured by using a chromameter (CS-100A, Minolta).

3. Results and discussion

The schematic structure diagrams of the OLEDs and the EODs used in this study are shown in Figs. 1 and 2. The EILs used in OLEDs I, II, and III are the Liq, the Cs_2CO_3, and the Cs_2CO_3/C_{60} layers, respectively. While the Li atoms or ions in the ETL diffused from the Liq EIL assist the electron mobility of the ETL [17], the Li atoms in the EML act as an exciton quenching site, resulting in a decrease in the luminance of the OLEDs. However, because the atomic weight of the Cs atom or ion is larger than that of the Li atom or ion, the magnitude of the diffusion of the Cs atoms or ions in the Cs_2CO_3 EIL is negligible in comparison with that of the Li

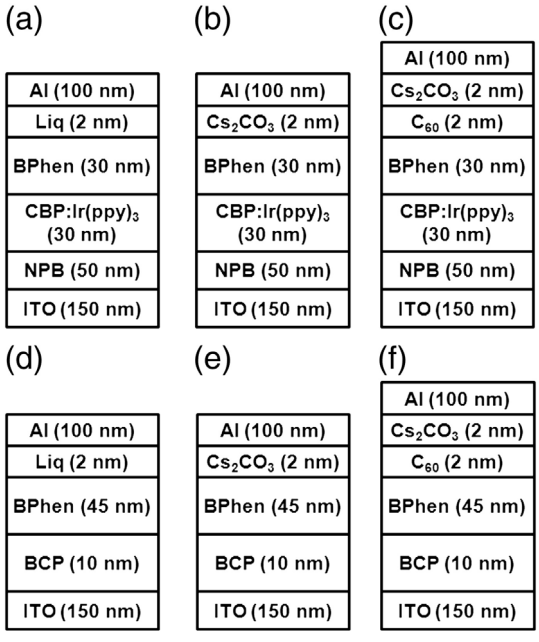

Fig. 1. Schematic diagrams for the OLEDs (a) I, (b) II, and (c) III and EODs (d) IV, (e) V, and (f) VI.

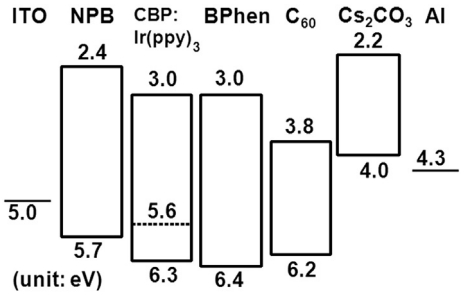

Fig. 2. Energy band diagram for the OLED III.

atoms or ions in the Liq EIL, resulting in a decrease of the number of the quenching sites as compared with that of the OLEDs with a Liq EIL. While the EILs and the ETLs of EODs IV, V, and VI are fabricated with the same structures of OLEDs I, II, and III, the BCP hole blocking layer (HBL) in EODs substitutes for the EML and the HTL of the OLEDs. Because the BCP HBL suppresses the hole injection from the ITO anode into the BPhen ETL under a low voltage, the current densities in EODs are attributed to the electrons injected through the EIL.

Fig. 2 shows the energy band diagram for OLED III. The C_{60} layer plays a role in acting a strong electron acceptor due to the low lowest unoccupied molecular orbital (LUMO) level of the C_{60} layer [18]. Because the negatively charged C_{60} layer attracts the holes injected from the BPhen ETL, the holes injected from the EML accumulate at the ETL/C_{60} heterointerface or in the C_{60} layer, acting as a hole blocking layer. While the holes in the EML at low operating voltages are effectively blocked by the BPhen ETL due to the low LUMO level of the BPhen layer, the BPhen ETL at high operating voltages cannot block efficiently the holes injected from the EML to the cathode. The C_{60} layer in OLED III at high operating voltages assists the hole blocking of the BPhen layer, resulting in an achievement of more balance of electrons and holes in the EML. Even though the LUMO level of Cs_2CO_3 is much higher than the workfunction of the Al cathode, the workfunction of the Cs_2CO_3/Al decreases to 2.2 eV due to the existence in the dipole moment of Cs_2CO_3, resulting in a decrease of the electron injection barrier [16].

Fig. 3 shows the current density–voltage characteristics for OLEDs I, II, and III. The current density of OLED I is smaller than those of OLEDs II and III. Because almost all of the CO_2 in the Cs_2CO_3 layer of OLED II outgases during evaporation process, the Cs layer forms at the interface between the BPhen ETL and the Al cathode. Some parts of Cs atoms or ions diffuse into the BPhen ETL or easily damage the surface of the BPhen ETL. However, the Cs atoms or ions in the OLEDs with a Cs_2CO_3 EIL or a Cs_2CO_3/C_{60} double EIL cannot diffuse deeply into the BPhen ETL due to the heavy atomic weight of Cs atoms. The C_{60} layer in the OLED III is used to protect the BPhen surface during a Cs_2CO_3

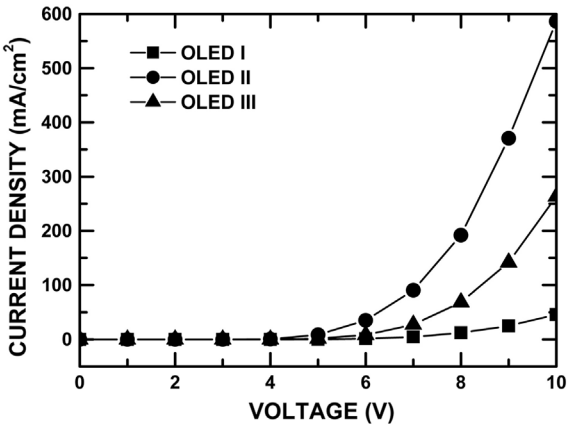

Fig. 3. Current density–voltage characteristics for the OLEDs I, II, and III.